Patch Recordings from the Electrocytes of *Electrophorus*

Na Channel Gating Currents

SCOTT SHENKEL and FRANCISCO BEZANILLA

From the Department of Cellular and Molecular Physiology, Yale University School of Medicine, New Haven, Connecticut 06510; the Department of Physiology, Ahmanson Laboratory of Neurobiology and Jerry Lewis Neuromuscular Research Center, University of California, Los Angeles, California 90024; and the Marine Biological Laboratory, Woods Hole, Massachusetts 02543

ABSTRACT Gating currents were recorded at 11°C in cell-attached and inside-out patches from the innervated membrane of *Electrophorus* main organ electrocytes. With pipette tip diameters of 3–8 μm, maximal charge measured in patches ranged from 0.74 to 7.19 fC. The general features of the gating currents are similar to those from the squid giant axon. The steady-state voltage dependence of the ON gating charge was characterized by an effective valence of 1.3 ± 0.4 and a midpoint voltage of −56 ± 7 mV. The charge vs. voltage relation lies ~30 mV negative to the channel open probability curve. The ratio of the time constants of the OFF gating current and the Na current was 2.3 at −120 mV and equal at −80 mV. Charge immobilization and Na current inactivation develop with comparable time courses and have very similar voltage dependences. Between 60 and 80% of the charge is temporarily immobilized by inactivation.

INTRODUCTION

Asymmetry currents have been attributed to the voltage-dependent gating transitions of Na channels (for review see Almers, 1978; Armstrong, 1981; Bezanilla, 1985). These tiny, rapid currents (gating currents) were first measured in the perfused squid giant axon (Armstrong and Bezanilla, 1973), and Na channel gating currents have since been studied in a variety of preparations: squid giant axon (Armstrong and Bezanilla, 1974, 1977; Keynes and Rojas, 1974; Meves and Vogel, 1977), frog node of Ranvier (Nonner et al., 1975), *Myxicola* giant axon (Rudy, 1976), crayfish giant axon (Swenson, 1980; Starkus et al., 1981), frog skeletal muscle (Collins et al., 1982; Campbell, 1983), canine cardiac Purkinje cells (Hanck et al., 1990), and *Xenopus* oocytes implanted with rat brain II Na channels (Conti and Stühmer, 1989).

The electric organ of *Electrophorus electricus* consists of the main organ, the Sachs

Address reprint requests to Dr. Scott Shenkel, Department of Cellular and Molecular Physiology, Yale University School of Medicine, 333 Cedar St., New Haven, CT 06510.

J. GEN. PHYSIOL. © The Rockefeller University Press · 0022-1295/91/09/0465/14 $2.00
Volume 98 September 1991 465–478

organ, and Hunter's organ. Within each organ the electrocytes are arrayed in rows and columns and are flattened in the anterior–posterior orientation. Only the innervated, posterior membrane is electrically excitable (Keynes and Martins-Ferreira, 1953), containing on the order of a few hundred Na channels per square micrometer in the main organ, as estimated from biochemical binding (Levinson, 1975) and electrophysiological (Shenkel and Sigworth, 1991) measurements. Also present are inward rectifying K channels (Nakamura et al., 1965), and nicotinic acetylcholine receptor channels (Popot and Changeux, 1984).

Shenkel and Sigworth (1991) have provided an initial characterization of *Electrophorus* electrocyte Na channels based on Na current recordings in patches from intact electrocytes from the Sachs and main electric organs. Due to the lack of contaminating ionic currents and the ability to measure both "macroscopic" and single-channel currents in membrane patches, the *Electrophorus* electrocyte appears to be an excellent preparation for the study of the functional properties of voltage-gated Na channels. Here we report the recording of Na channel gating currents from cell-attached and inside-out patches from main organ electrocytes. Na channel ionic currents are presented for comparison with the gating currents. The general properties of the gating currents are comparable to those previously measured in nerve and muscle preparations.

A preliminary account of these data has been published (Shenkel and Bezanilla, 1990).

METHODS

The experiments were performed at 11°C on freshly dissected electroytes from the main electric organ of *Electrophorus*. The preparation, electrocyte dissection, and patch-recording of Na currents were performed according to the methods previously described (Shenkel and Sigworth, 1991), the only major differences being the larger pipette tip diameters to resolve gating currents and the lower temperature used here. Patch pipettes were fabricated (Hamill et al., 1981) from KIMAX-51 (Kimble Glass Inc., Vineland, NJ) or Corning 7052 (Garner Glass Co., Claremont, CA) glass capillaries with tip diameters ranging from 3 to 8 μm. Pipette resistances were 0.3–1.7 MΩ. Recordings were made in either the cell-attached or the inside-out patch configuration. To record gating currents all permeant ions were replaced with the impermeant cation *N*-methylglucamine and tetrodotoxin was added to the pipette to block any residual current through Na channels. Pipette and bath solutions for measuring ionic and gating currents are listed in Table I.

Linear capacitive current cancellation and leak subtraction were performed using either P/4 or P/−4 pulses (Bezanilla and Armstrong, 1977) from a subtracting holding potential (SHP) of −140 mV (gating current measurements) or −120 mV (ionic current measurements). The current monitor signal from an integrating patch clamp (model 3900; Dagan Corp., Minneapolis, MN) was low-pass filtered at 20 or 10 kHz with an 8-pole Bessel filter and sampled by a 15-bit A/D converter (MP2735; Analogic Corp., Peabody, MA) at 6 μs (for gating and instantaneous currents) or 10 μs (for Na current traces used for obtaining peak currents and inactivation time constants) per point. Under these filtering conditions the rapid time course of some of the currents may have been distorted, since even at 10 kHz the filter rise time is ~30 μs. Typically, 20–40 gating current traces were averaged for display and analysis to improve the signal-to-noise ratio. The gating charge was calculated by digitally integrating the current records for 1–2 ms after the start of the pulse.

TABLE I

*Solutions**

Component	Ionic		Gating	
	Pipette	Bath	Pipette	Bath
			mM	
Na	200	—	—	—
K	—	200	—	—
Ca	3	—	3	—
Mg	1.5	2	1.5	2
EGTA‡	—	1	—	1
HEPES§	5	5	5	5
NMG‖	—	—	200	200
TTX¶	—	—	400×10^{-6}	—

*Chloride salts. pH 7.2–7.4.
‡Ethylene glycol-bis (β-aminoethylether) *N,N,N′,N′*-tetraacetic acid
§*N*-2-hydroxyethylpiperazine-*N′*-2-ethanesulfonic acid
‖*N*-Methylglucamine
¶Tetrodotoxin

RESULTS

Gating Current Traces

Fig. 1 shows a family of gating currents (I_g) recorded in a cell-attached patch. The average of 20 sweeps is shown for each potential after P/−4 subtraction. Depolarizing pulses were preceded by a 20-ms hyperpolarizing prepulse to −120 mV from a holding potential of −90 mV. After a step depolarization, the ON gating current (I_g ON) rises rapidly to a peak and decays in at least two distinct phases. I_g ON becomes

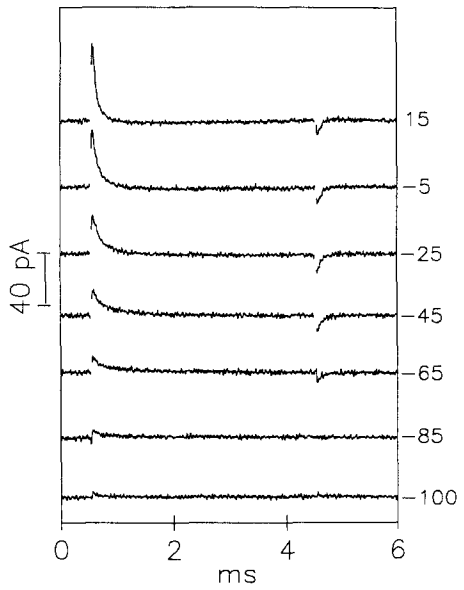

FIGURE 1. A family of I_g traces recorded in a cell-attached patch. Currents were elicited by step depolarizations of 4 ms duration to the indicated voltages. Pulses were applied at 0.3-s intervals after a 20-ms hyperpolarizing prepulse to −120 mV from a holding potential of −90 mV. The first and last 30 μs of traces corresponding to voltages between −65 and +15 mV were blanked out. P/−4 pulses with SHP = −140 mV. Filter, 15 kHz. Temperature, 11°C.

larger and faster with increasing depolarization; the time constant of the fast component decreased from ~120 to 70 μs in the voltage range −65 to +15 mV. At the end of the 4-ms pulse, OFF gating current (I_g OFF) was observed upon return of the potential to −90 mV from voltages more positive than −85 mV; no I_g OFF was detected after pulses to −85 and −100 mV due to the small difference between the amplitude of the depolarizing pulses and the return potential. I_g OFF rises quickly and is smaller than I_g ON. The smaller size is partly due to the difference between the

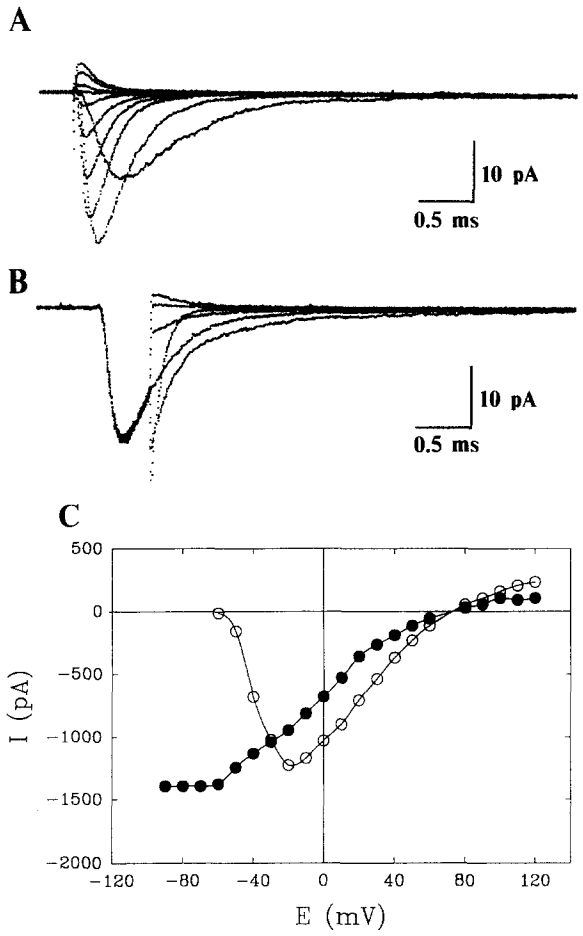

FIGURE 2. Families of current traces used to determine (*A*) I_p and (*B*) I_{inst} recorded in an inside-out patch, and (*C*) current–voltage relations. (*A*) Peak currents are shown for step depolarizations of 4 ms duration in the voltage range −60 to +120 mV in 20-mV increments. (*B*) I_{inst} are shown for voltage steps in the range −80 to +120 mV in 40-mV increments after a 0.5-ms step depolarization to 0 mV. A 20-ms hyperpolarizing prepulse to −120 mV preceded each depolarizing step in *A* and *B*. Holding potential, −90 mV. P/−4 pulses with SHP = −120 mV. Filter, 10 kHz. Temperature, 11°C. (*C*) I_p- (*open circles*) and I_{inst}-voltage relations (*filled circles*) for the experiments of *A* and *B*.

return (−90 mV) and prepulse (−120 mV) potentials, but mainly to the temporary immobilization of the gating charge (Armstrong and Bezanilla, 1977). We suspect that the immobilized component of the charge is too small and returns too slowly at this voltage to be seen above the baseline noise. I_g OFF decay transients were well fitted by a single exponential function with a time constant near 70 μs.

Charge–Voltage Relationships

The charge vs. voltage (*Q-V*) curve lies ~30 mV to the left of the channel open probability vs. voltage (P_o-*V*) curve. At each potential, an estimate of P_o was obtained

from the ratio of the peak (Fig. 2 *A*) and instantaneous currents (Fig. 2 *B*) as described in Stimers et al. (1985), except inactivation was not removed in our experiments. The peak (I_p) and instantaneous (I_{inst}) currents are plotted as a function of voltage in Fig. 2 *C*. The voltage dependence of P_o is shown in Fig. 3 as the open symbols. P_o increases steeply in the voltage range −65 to −40 mV and then more gradually at stronger depolarizations.

The total ON gating charge Q_{ON} (closed symbols in Fig. 3) was obtained at each potential by integrating the I_g ON traces over 1–2 ms from the start of the pulse. A considerable amount of charge is moved in the region −110 to −65 mV, a region where P_o is very small. The maximal charge (Q_{max}) measured in this patch was 6.5 fC

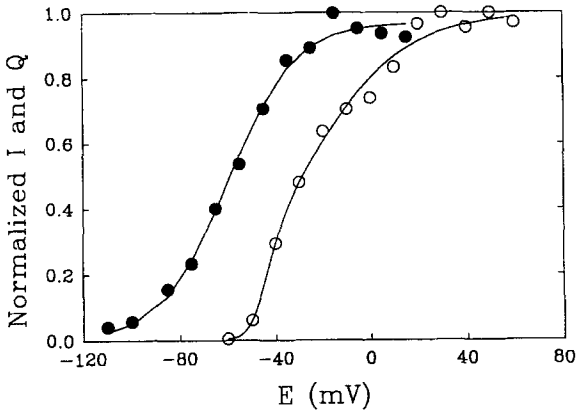

FIGURE 3. Comparison of Q vs. V (*filled circles*) and P_o vs. V curves (*open circles*). Q_{ON} and I_p were measured during depolarizing voltage steps after a 20-ms hyperpolarizing prepulse to −120 mV from a holding potential of −90 mV. The solid line through the Q data was obtained from a least-squares fit of a Boltzmann function

$$\frac{Q_{ON}}{Q_{max}} = \frac{1}{1 + \exp(-zF(E - E_q)/RT)}$$

where the valence of the elementary gating charge $z = 1.8$ and the midpoint voltage $E_q = -60$ mV. R, T, and F are the gas constant, absolute temperature, and the Faraday constant, respectively. At each potential, P_o was obtained as the normalized ratio of I_p and I_{inst} (see Results).

($\sim 40 \times 10^3$ elementary charges). Assuming four to six elementary charges per channel and a patch area of ~ 200 μm^2 (pipette tip diameter = 5 μm), this amount of charge corresponds to $\sim$35–50 channels/μm^2. This is within the range of $\sim$10–100 channels/μm^2 estimated from variance–mean analysis of macroscopic Na currents recorded in membrane patches from Sachs organ electrocytes (Shenkel and Sigworth, 1991), but less than the estimate obtained by Levinson (1975; biochemical binding) of ~ 500 μm^{-2}.

The solid line drawn through the Q data points is a least-squares fit of a Boltzmann function (see legend for parameters). Fitted curves were used to obtain an estimate

for the midpoint potential (E_q) of the Q-V relationships and are summarized in Table II from different patches. The valence of the gating charge (z_q) was obtained from the initial rise of the Q-V relation at very negative potentials (Almers, 1978). On a semilogarithmic plot it was determined that the charge rises exponentially in the voltage region −70 to −110 mV. At more negative potentials the currents were too small to obtain reliable amplitude estimates. Values of z_q were obtained from the slope of a linear least-squares fit to typically four or five Q data points in this region and are given in Table II. Also summarized in Table II are Q_{max} and the number of channels in a patch N.

TABLE II

Summary of Steady-State Q-V Parameters

File	Cell	Patch*	z_q	E_q	Q_{max}‡	Diameter§	N‖
				mV	*fC*	μm	
SE089A	1	1 (A)	2.4	−65	0.74	3	900
		2 (A)	1.3	−62	1.51	3	1,900
		3 (A)	1.3	−60	6.50	5	8,100
SE119A	2	1 (D)	1.4	−47	0.91	3	1,100
		2 (D)	1.1	−48	1.83	3	2,300
SE139A	3	1 (A)	1.0	−63	4.63	5	5,800
		2 (A)	1.2	−62	7.19	7	9,000
		3 (A)	1.3	−60	7.15	8	8,900
	4	1 (A)	1.1	−44	2.11	3	2,600
		1 (D)	1.2	−58	1.63	3	2,000
		2 (A)	0.8	−51	3.10	4	3,900
	5	1 (A)	1.3	−57	2.70	7	3,400
Mean ± SD			1.3 ± 0.4	−56 ± 7 mV			

*Patch number per cell A = cell-attached and D = detached (inside-out).

‡Q_{max} was taken as the largest Q value obtained over a range of potentials and was typically observed near 0 mV.

§Pipette tip diameter.

‖The number of channels N was estimated from $N = Q_{max}/z_a e$, where the elementary charge $e = 1.6 \times 10^{-19}$ C, and the valence z_a of the effective gating charge for opening each channel was assumed to be 5. Estimates of N were rounded to the nearest 100 channels.

Time Courses

Fig. 4 compares the time courses of I_g and Na current (I_{Na}) for identical pulse patterns. After a step depolarization to 0 mV most of the I_g flows before the peak of the inward I_{Na} (Fig. 4, *A* and *B*). Upon repolarization to −120 mV (Fig. 4 *A*) the time constant of the I_g OFF transient was 2.3 times larger than the decay transient of I_{Na}. However, at −80 mV the time constants were equal (Fig. 4 *B*). Intermediate values of 1.7 and 2.0 were obtained for repolarization potentials of −100 and −110 mV, respectively.

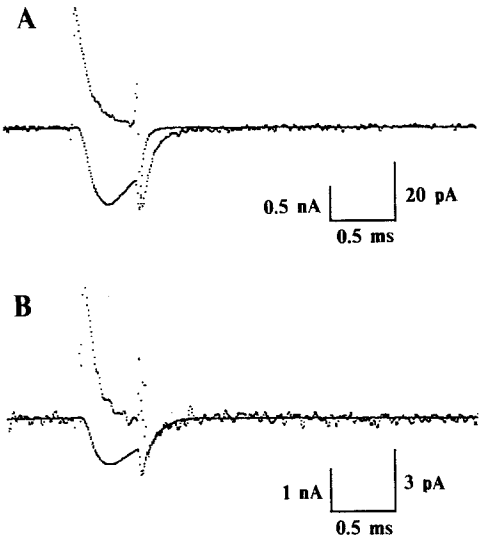

FIGURE 4. Comparison of I_g and I_{Na} activation at 0 mV and deactivation at −120 mV (*A*) and −80 mV (*B*). The I_g current is the noisy trace in *A* and *B*. Depolarizations to 0 mV of 0.5 ms duration were preceded by a 20-ms hyperpolarizing prepulse to −120 mV. Holding potential, −90 mV. The decay time constants were (in microseconds): 70 (I_g) and 30 (I_{Na}) at −120 mV; 95 (I_g) and 92 (I_{Na}) at −80 mV. P/−4 pulses with SHP = −140 mV (I_g) and −120 mV (I_{Na}). Filter, 10 kHz. Temperature, 11°C.

Charge Immobilization: Time Course

Charge immobilization and I_{Na} inactivation have similar time courses. Fig. 5 shows superimposed I_g ON traces for pulses to 0 mV after a 20-ms prepulse to −120 mV from a holding potential of −90 mV. After various durations (given in milliseconds) I_g OFF were recorded upon repolarization to the same potential as the prepulse, −120 mV. I_g OFF declined as the pulse duration increased above ~0.3 ms and reached a steady level for durations greater than ~1.5 ms. The time course of the decline of the OFF/ON charge ratio (Fig. 6) was well fitted by a single exponential with a time constant of 0.62 ms and a final value of 0.2 for the data of Fig. 5. In the same patch but with a test potential of +20 mV, the OFF/ON ratio declined to the same final value but with a time constant of 0.37 ms. The inset to Fig. 6 shows a typical inward I_{Na} recording obtained at 0 mV; its inactivation time constant τ_h is 0.74 ms. The time constants of charge immobilization were within the range of values observed for the

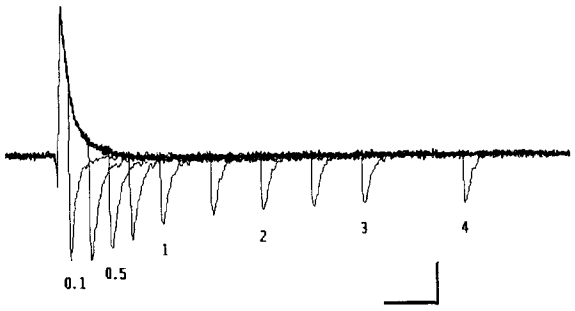

FIGURE 5. A sequence of I_g traces recorded at various pulse durations. Currents were elicited by voltage steps to 0 mV and after various durations (given in milliseconds), the patch membrane was repolarized to −120 mV. Depolarizing voltage steps were preceded by a 20-ms prepulse to −120 mV from a holding potential of −90 mV. The average of 20 sweeps is shown for each superimposed trace. The scale bars correspond to 0.5 ms and 10 pA. P/−4 pulses with SHP = −140 mV. Filter, 10 kHz. Temperature, 11°C.

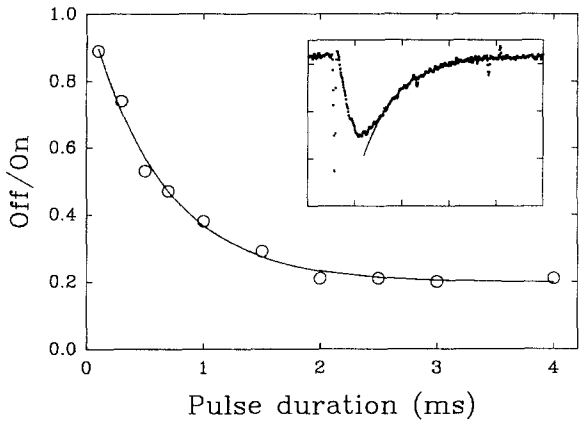

FIGURE 6. Time course of the OFF/ON charge ratio as a function of pulse duration. Same experiment as in Fig. 5. The solid curve was drawn according to

$$\text{OFF/ON} = \exp(-t/\tau) + c$$

where the immobilization time constant τ and the final value c are given in the text. (*Inset*) I_{Na} recorded at 0 mV after a 20-ms prepulse to −120 mV from a holding potential of −90 mV. The intervals between vertical and horizontal tic marks correspond to 100 pA and 1 ms, respectively. P/−4 pulses with SHP = −120. Filter, 10 kHz. Temperature, 11°C.

decay of the Na current during maintained depolarizations (Table III). The amount of scatter in τ_h among patches observed here was similar to that previously reported by Shenkel and Sigworth (1991).

Charge Immobilization: Voltage Dependence

Charge immobilization and I_{Na} inactivation have very similar voltage dependences. The steady-state voltage dependence of electrocyte Na current inactivation was studied by Shenkel and Sigworth (1991) using a two-pulse protocol method (Hodgkin and Huxley, 1952). The same procedure was used here to investigate the voltage dependence of charge immobilization. Q_{ON} and peak Na current I_t were measured in separate patches during a test pulse to either +10 mV (Q_{ON}) or 0 mV (I_t) after conditioning prepulses E_p of varying potential and 20-ms duration from a holding potential of −90 mV. A brief pulse of 0.3 or 0.5 ms to the holding potential was inserted between the prepulse and the test pulse in the gating current experiments.

TABLE III

Na Current Inactivation Time Constants (ms) at Three Different Voltages

File	Cell	−30 mV	0 mV	+20 mV
SE049A	1	0.51	0.31	0.29
	2	1.30	0.95	1.10
SE069A	3	0.46	0.28	0.35
SE089A	4	0.90	0.66	0.84
	5	0.59	0.33	0.31
SE119B	6	0.91	0.56	0.40
SE139A	7	0.75	0.68	0.92
Mean ± SD		0.77 ± 0.31	0.54 ± 0.24	0.60 ± 0.34

Currents were measured during step depolarizations to the indicated voltages after a 20-ms hyperpolarizing prepulse to −120 mV from a holding potential of −90 mV. The decay phase of each current was well fitted by a single exponential function with the indicated time constant. Temperature, 11°C.

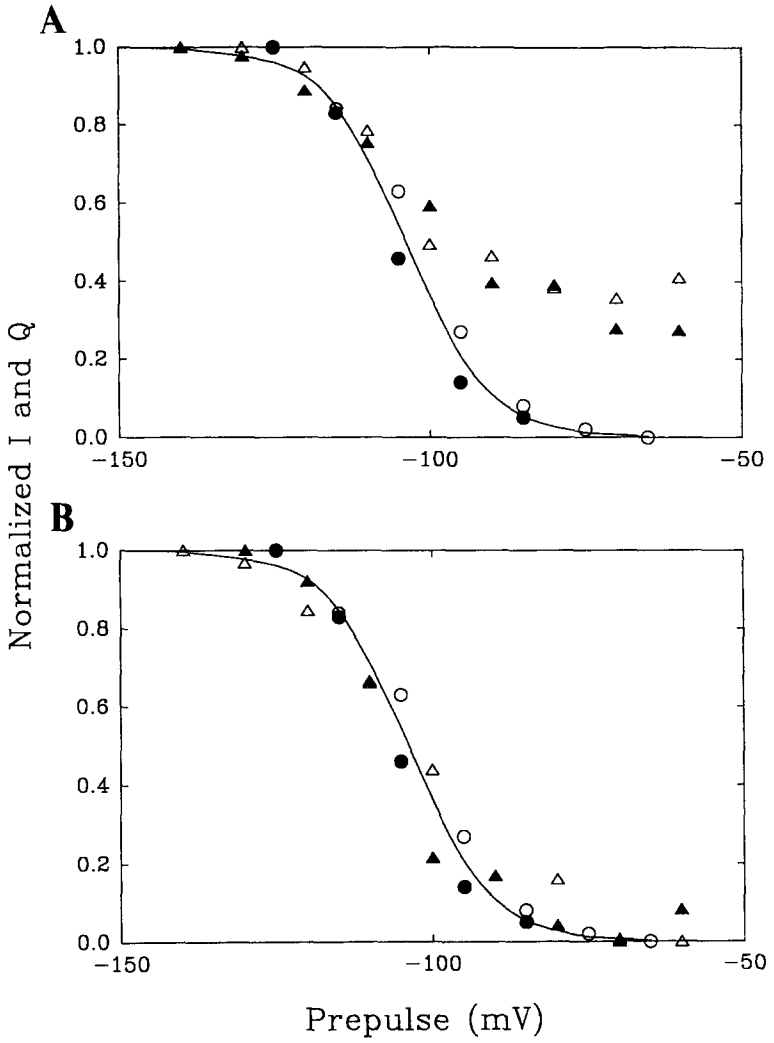

FIGURE 7. Comparison of the steady-state voltage dependence of charge immobilization and I_{Na} inactivation before (*A*) and after (*B*) rescaling of the charge data. The I_{Na} data are from Shenkel and Sigworth (1991) and correspond to their main organ electrocytes no. 1 (*open circles*) and no. 6 (*filled circles*) recorded at 22–24°C. The solid curve is a least-squares fit of a Boltzmann function

$$\frac{I_t}{I_{max}} = \frac{1}{1 + \exp(z_h F(E_p - E_h)/RT)}$$

where the valence of the apparent inactivation gating charge z_h = 3.8 and the inactivation midpoint voltage E_h = −104 mV.

Q_{max} and maximal Na current (I_{max}) were typically obtained with E_p between −130 and −120 mV. With more positive E_p the ratios Q_{ON}/Q_{max} and I_t/I_{max} declined as illustrated in Fig. 7 *A* for two representative gating (triangles) and Na current (circles) experiments; filled and open symbols correspond to different patches from different cells. With increasingly positive prepulses I_t decreased to zero, whereas Q_{ON} declined to a steady value of 30%. The solid curve is a least-squares fit of a Boltzmann function to the average of the I_{Na} data (see legend for parameters). A closer comparison of the steady-state voltage dependence of charge immobilization and I_{Na} inactivation is shown in Fig. 7 *B*, in which the normalized charge data were replotted after subtraction of the nonimmobilized portion of the charge.

DISCUSSION

We have presented here an initial characterization of *Electrophorus* electrocyte Na channel I_g based on patch clamp recordings from the innervated membrane of intact main organ electrocytes. We have found that the general features of the I_g are similar to those measured in the squid giant axon and other preparations.

After a step depolarization the eel electrocyte Na channel I_g rose quickly to a peak and decayed in at least two distinct phases, similar to the behavior of I_g in the squid giant axon. In squid, I_g ON rises in <10 μs (Stimers et al., 1987) and decays with a fast and intermediate component in the voltage range −20–0 mV (Armstrong and Bezanilla, 1977; Armstrong and Gilly, 1979). At more depolarized voltages, I_g has a third slower phase which might not be associated with Na channel gating (Armstrong and Gilly, 1979).

We did not detect a component of I_g with a time constant comparable to τ_h; the time constant of the slowest component of I_g was at least twofold smaller than τ_h at the same potential. Similar results have been found in squid axon (Armstrong and Bezanilla, 1977). Only in crayfish axon has a component of I_g been found with a time constant similar to τ_h (Swenson, 1983).

For the eel Na channels the steady-state voltage dependence of the charge movement was well fitted by a simple Boltzmann function. The *Q-V* relation in squid axon has also been fitted with a Boltzmann function (Keynes and Rojas, 1974), but more recent work in squid has revealed a "bump" of extra charge at voltages more negative than −70 mV (Bezanilla and Armstrong, 1976) which appears to be associated with charge movement among closed states of the channel (Taylor and Bezanilla, 1983). This extra charge appears to be absent from our *Q-V* curves.

We obtained a minimum effective valence of ~1.3 for the elementary Na channel gating charge. Our estimate is within the range of values 0.9–2.4 for the gating charge based on reports from nerve (Keynes and Rojas, 1974; Nonner et al., 1975; Rudy, 1976; Chiu, 1980; Starkus et al., 1981), skeletal muscle (Collins et al., 1982; Campbell, 1983), cardiac (Hanck et al., 1990), and oocyte (Conti and Stühmer, 1989) preparations. Conti and Stühmer (1989) obtained an estimate of 2.3 for the elementary gating charge from I_g fluctuation measurements in rat II Na channels expressed in *Xenopus* oocytes. Using the same analysis performed on one patch with ~600 traces at 0 mV and a bandwidth of 10 kHz we determined a valence for the elementary gating charge of 1.8.

The *Q-V* curve lies ~30 mV to the left of the P_o-*V* curve, indicating that there is a

sizable amount of charge moving among closed states. Our estimates of P_o were obtained from the ratio of I_p and I_{inst} at each voltage, assuming that P_o approaches 1 at E $\geq$ +40 mV. Shenkel and Sigworth (1991) found from fluctuation analysis that the midpoint of the absolute P_o-V curve probably lies further to the right, with a midpoint of ~3 mV. Both in our determination and in the determination of Shenkel and Sigworth the P_o represents the fraction of channels conducting at the peak of the Na current and is thus not a direct measure of the degree of activation of the channels at the test potential. Stimers et al. (1985) found that in squid the P_o-V curve rises less steeply (but the Q-V curve is not significantly different) after removal of inactivation with Pronase; in this case the midpoint voltages of the Q-V and P_o-V curves were −30 and −15 mV, respectively. In the normal axon with inactivation intact, the P_o-V has a center point near −20 mV; the difference between the P_o-V midpoints is probably due to the error caused by using the peak current to estimate P_o when inactivation is present (Stimers et al., 1985). The uncertainty in the determination of the P_o-V curve in the present work due to the presence of the inactivation process precludes a definitive comparison between the Q-V and the P_o-V curves, but it is clear that the Q-V curve is displaced far to the left of the P_o-V curve. A quantitative comparison of Q-V and P_o-V will require experiments performed in electrocytes with inactivation removed (Stimers et al., 1985). However, it does appear that in the eel channel there is a much larger difference between the midpoints of the two curves.

Our results from the comparison of the decay transients of I_{Na} and I_g during identical pulse patterns are inconsistent with models based on a set of three or more identical independent gating particles (Bezanilla and Armstrong, 1975). Upon return of the membrane potential to −80 mV after a depolarizing pulse, the decay time constants of I_g OFF and I_{Na} were equal. Only for more negative return potentials did the ratio of time constants become greater than one; at −110 mV, I_g OFF decayed two times more slowly than I_{Na}. Qualitatively similar results were found in squid where the ratio of the I_g OFF and I_{Na} decay time constants is 1 at −60 mV and reaches a maximum value of 1.7 at −110 mV (Armstrong and Bezanilla, 1977).

The phenomenon of charge immobilization was found in the squid (Armstrong and Bezanilla, 1974) and served as a basis to correlate inactivation and activation with the same set of gating particles. The time course and voltage dependence for charge immobilization and I_{Na} inactivation were found to be the same, which led to the proposal that I_{Na} inactivation results from the temporary immobilization of the gating charge (Armstrong and Bezanilla, 1977). These authors found that 60–70% of the charge became immobilized with pulses to ~0 mV. Similar results have been reported for crayfish giant axons (Swenson, 1980), frog node of Ranvier (Nonner, 1980), and frog skeletal muscle (Campbell, 1983). However, a lack of correlation between charge immobilization and I_{Na} inactivation has been reported in squid (Meves and Vogel, 1977) and *Myxicola* (Bullock and Schauf, 1979) giant axons. In the present report we found that the value of τ_h, measured from the decay of I_{Na} during maintained depolarizations, varied by as much as a factor of 3 among patches at the same potential (Table III), and no systematic difference in τ_h was observed between cell-attached and inside-out patches. Similar results have been reported by Shenkel and Sigworth (1991). We found that the time constant of charge immobilization was

in the observed range of τ_h values. Furthermore, charge immobilization and I_{Na} inactivation had very similar voltage dependences, although inactivation decreased I_{Na} to zero, while the charge declined to 20–40%. The relationship between charge immobilization and I_{Na} inactivation is therefore qualitatively similar to the results reported by Armstrong and Bezanilla (1977) in squid, except that the voltage dependence of both processes is displaced to more negative potentials in the electrocytes with midpoints near −95 mV.

The intact electrocyte preparation has a high density of Na channels that has allowed us to record gating currents with very good signal-to-noise ratio. The density is also appropriate to record gating current fluctuations. The properties of the gating currents show close similarity to the gating currents of the squid giant axon with quantitative differences in the voltage dependence of activation and inactivation. In this preparation it is also possible to record macroscopic and single channel ionic currents. Considering that much of the biochemistry (Agnew et al., 1988) and reconstitution (Rosenberg et al., 1984; Recio-Pinto et al., 1987; Shenkel et al., 1989; Correa et al., 1990) has been done on the eel Na channel, and that its primary structure is known (Noda et al., 1984), makes this preparation ideal for the study of the function of Na channels in situ.

We thank Fred Sigworth for encouragement and helpful comments on the manuscript, and Bill Agnew for supplying *Electrophorus*.

This work was supported by NIH grants GM-30376, NS-17928, and NS-21501.

Original version received 21 May 1990 and accepted version received 19 April 1991.

REFERENCES

Agnew, W. S., E. C. Copper, W. M. James, S. A. Tomiko, R. L. Rosenberg et al. 1988. Voltage-sensitive sodium channels: molecular structure and function. *Current Topics in Membranes and Transport.* 33:329–365.

Almers, W. 1978. Gating currents and charge movements in excitable membranes. *Reviews of Physiology, Biochemistry and Pharmacology.* 82:96–190.

Armstrong, C. M. 1981. Sodium channels and gating currents. *Physiological Reviews.* 61:644–683.

Armstrong, C. M., and F. Bezanilla. 1973. Currents related to movements of the gating particles of the Na channels. *Nature.* 242:459–461.

Armstrong, C. M., and F. Bezanilla. 1974. Charge movement associated with opening and closing of the activation gates of the Na channels. *Journal of General Physiology.* 63:533–552.

Armstrong, C. M., and F. Bezanilla. 1977. Inactivation of the sodium channel. II. Gating current experiments. *Journal of General Physiology.* 70:567–590.

Armstrong, C. M., and W. F. Gilly. 1979. Fast and slow steps in the activation of sodium channels. *Journal of General Physiology.* 74:691–711.

Bezanilla, F. 1985. Gating of sodium and potassium channels. *Journal of Membrane Biology.* 88:97–111.

Bezanilla, F., and C. M. Armstrong. 1976. Properties of the sodium channel gating current. *Cold Spring Harbor Symposia on Quantitative Biology.* 40:297–304.

Bezanilla, F., and C. M. Armstrong. 1977. Inactivation of the sodium channel. I. Sodium current experiments. *Journal of General Physiology.* 70:549–566.

Bullock, J. O., and C. L. Schauf. 1979. Immobilization of intramembrane charge in *Myxicola* giant axons. *Journal of Physiology.* 286:157–171.

Campbell, D. T. 1983. Sodium channel gating currents in frog skeletal muscle. *Journal of General Physiology.* 82:679–701.

Chiu, S. Y. 1977. Asymmetry currents in the mammalian myelinated nerve. *Journal of Physiology.* 309:499–519.

Collins, C. A., E. Rojas, and B. A. Suarez-Isla. 1982. Fast charge movements in skeletal muscle fibers from *Rana temporaria. Journal of Physiology.* 324:319–345.

Conti, F., and W. Stühmer. 1989. Quantal charge redistributions accompanying the structural transitions of sodium channels. *European Biophysical Journal.* 17:53–59.

Correa, A. M., F. Bezanilla, and W. S. Agnew. 1990. Voltage activation of purified eel sodium channels reconstituted into artificial liposomes. *Biochemistry.* 29:6230–6240.

Hamill, O. P., A. Marty, E. Neher, B. Sakmann, and F. J. Sigworth. 1981. Improved patch-clamp techniques for high resolution current recording from cells and cell-free membrane patches. *Pflügers Archiv.* 391:85–100.

Hanck, D. A., M. F. Sheets, and H. A. Fozzard. 1990. Gating currents associated with Na channels in canine cardiac Purkinje cells. *Journal of General Physiology.* 95:439–457.

Hodgkin, A. L., and A. F. Huxley. 1952. A quantitative description of membrane current and its application to conduction and excitation in nerve. *Journal of Physiology.* 117:500–544.

Keynes, R. D., and H. Martins-Ferreira. 1953. Membrane potentials in the electroplates of the electric eel. *Journal of Physiology.* 119:315–351.

Keynes, R. D., and E. Rojas. 1974. Kinetics and steady-state properties of the charged system controlling sodium conductance in the squid giant axon. *Journal of Physiology.* 239:393–434.

Levinson, S. R. 1975. Studies on excitable membranes. Ph.D. Dissertation. University of Cambridge, Cambridge, UK. 199 pp.

Meves, H., and W. Vogel. 1977. Inactivation of the asymmetrical displacement current in giant axons of *Loligo forbesi. Journal of Physiology.* 267:377–393.

Nakamura, Y., S. Nakajima, and H. Grundfest. 1965. Analysis of spike electrogenesis and depolarizing K inactivation in electroplaques of *Electrophorus electricus,* L. *Journal of General Physiology.* 49:321–349.

Noda, M., S. Shimizu, T. Tanabe, T. Takai, T. Kayano, et al. 1984. Primary structure of *Electrophorus electricus* sodium channel deduced from cDNA sequence. *Nature.* 312:121–127.

Nonner, W. 1980. The relations between the inactivation of sodium channels and the immobilization of gating charge in frog myelinated nerve. *Journal of Physiology.* 299:573–603.

Nonner, W., E. Rojas, and R. Stämpfli. 1975. Displacement currents in the node of Ranvier: voltage and time dependence. *Pflügers Archiv.* 354:1–18.

Popot, J. L., and J. P. Changeux. 1984. Nicotinic receptor of acetylcholine: structure of an oligomeric integral membrane protein. *Physiological Reviews.* 64:1162–1239.

Recio-Pinto, E., D. S. Duch, S. R. Levinson, and B. W. Urban. 1987. Purified and unpurified sodium channels from eel electroplax in planar lipid bilayers. *Journal of General Physiology.* 90:375–395.

Rosenberg, R. L., S. A. Tomiko, and W. S. Agnew. 1984. Single channel properties of the reconstituted voltage-regulated Na channel isolated from the electrocytes of *Electrophorus electricus. Proceedings of the National Academy of Sciences, USA.* 81:5594–5598.

Rudy, B. 1976. Sodium gating currents in *Myxicola* giant axons. *Proceedings of the Royal Society of London, B.* 193:469–475.

Shenkel, S., and F. Bezanilla. 1990. Gating currents in electrocyte Na channels of the electric eel *E. electricus. Biophysical Journal.* 57:102*a*. (Abstr.)

Shenkel, S., E. C. Cooper, W. James, W. S. Agnew, and F. J. Sigworth. 1989. Purified, modified eel sodium channels are active in planar bilayers in the absence of activating neurotoxins. *Proceedings of the National Academy of Sciences, USA.* 86:9592–9596.

Shenkel, S., and F. J. Sigworth. 1991. Patch recordings from the electrocytes of *Electrophorus electricus*. Na currents and P_{Na}/P_K variability. *Journal of General Physiology.* 97:1013–1041.

Starkus, J. G., B. D. Fellmeth, and M. D. Rayner. 1981. Gating currents in the intact crayfish giant axon. *Biophysical Journal.* 35:521–533.

Stimers, J. R., F. Bezanilla, and R. E. Taylor. 1985. Sodium channel activation in the squid giant axon. Steady-state properties. *Journal of General Physiology.* 85:65–82.

Stimers, J. R., F. Bezanilla, and R. E. Taylor. 1987. Sodium channel gating current. Origin of the rising phase. *Journal of General Physiology.* 89:521–540.

Swenson, R. P. 1980. Gating charge immobilization and sodium current inactivation in internally perfused crayfish axons. *Nature.* 287:644–645.

Swenson, R. P. 1983. A slow component of gating current in crayfish giant axons resembles inactivation charge movement. *Biophysical Journal.* 41:245–249.

Taylor, R. E., and F. Bezanilla. 1983. Sodium channel and gating current time shifts resulting from changes in initial conditions. *Journal of General Physiology.* 81:773–784.